Interactions between Diphenylcarbazide, Zinc, Cobalt, and Manganese on the Oxidizing Side of Photosystem II†

Maria L. Ghirardi, Thomas W. Lutton, and Michael Seibert*

Photoconversion Branch, National Renewable Energy Laboratory, Golden, Colorado 80401

Received July 19, 1995; Revised Manuscript Received December 4, 1995⊗

ABSTRACT: The inhibition of DPC-mediated DCIP photoreduction by exogenous $MnCl_2$ in Tris-treated photosystem II (PSII) membrane fragments has been used to probe for amino acids on the PSII reaction center proteins, including D1His337, that provide ligands for binding manganese [Preston, C., & Seibert, M. (1990) in *Current Research in Photosynthesis* (Baltscheffsky, M., Ed.) Vol. I, pp 925−928, Kluwer Academic Publishers, Dordrecht, The Netherlands; Preston, C., & Seibert, M. (1991) *Biochemistry 30*, 9615−9624 and 9625−9633]. At a concentration of 200 μM, DPC is photooxidized at both a high-affinity and a low-affinity site in PSII at approximately the same initial rate. Addition of 10 μM $MnCl_2$ noncompetitively inhibits DPC photooxidation at the high-affinity site, with a K_i of 1.5 μM, causing a decrease of about 50% in the overall DCIP photoreduction rate. The high-affinity site for Mn binding was deconvoluted into four independent components. In earlier work, the inhibition was attributed to the tight association of either Mn^{2+} or Mn^{3+} with the PSII membrane. We report here that inhibition of DPC photooxidation may involve two different types of high-affinity, Mn-binding components: (a) one that is specific for Mn, and (b) others that bind Mn, but may also bind additional divalent cations, such as Zn and Co, that are not photooxidized by PSII. These conclusions are based on the observations that (a) DPC photooxidation can be inhibited by Zn^{2+} and Co^{2+}; (b) Zn^{2+} and Co^{2+} interact with Mn^{2+} in a nonmutually exclusive manner, suggesting that they may share some binding components with Mn^{2+}; (c) high-affinity Mn^{2+} (but not Zn^{2+} or Co^{2+}) inhibition of DPC photooxidation is accompanied by nondecaying fluorescence emission, following a single saturating flash, indicating efficient electron donation by Mn^{2+} to Y_Z^+; (d) Mn^{2+} photooxidation in the presence of DPC is not inhibited by Zn^{2+} or Co^{2+}; and (e) kinetic modeling of the interaction between high-affinity Mn^{2+} and DPC in PSII indicates inhibition of *steady-state* Mn^{2+} photooxidation by DPC, but allows for a single photooxidation of Mn^{2+}. We conclude that Mn inhibition of DPC photooxidation can be used to identify Mn-binding sites of physiological importance, and suggest that the Mn-specific component of the high-affinity, Mn-binding site involves the ligand to the first Mn bound during photoactivation (i.e., Asp170 on D1, as found by other investigators).

Primary charge separation in photosystem II (PSII)[1] generates a strong oxidant, P_{680}^+, in about 3 ps [see Seibert (1993) for a review], that is subsequently reduced by Tyr161 on the D1 protein (Debus et al., 1988; Metz et al., 1989). The resulting oxidized tyrosine radical, Y_Z^+, is then re-reduced by electrons ultimately obtained from H_2O. Electron transfer from H_2O to Y_Z^+ is mediated by a tetrameric manganese cluster (Cheniae & Martin, 1971) bound to the reaction center (RC) proteins of PSII (Metz et al., 1986; Coleman & Govindjee, 1987; Dismukes, 1988). Alternative donors to P_{680}^+, such as Y_D (Tyr160 on the D2 protein; Debus et al., 1988; Vermaas et al., 1988; Buser et al., 1990; Barry, 1993) and cytochrome b_{559} (cyt b_{559}; Thompson & Brudvig, 1988; Miller & Brudvig, 1990), have also been described. However, they are photooxidized with low yields at room temperature in O_2-evolving PSII preparations (Styring & Rutherford, 1987; Buser et al., 1990).

Information about specific amino acid residues that provide ligands for Mn in PSII has been examined using two approaches. One approach is based on the construction of site-directed mutants in *Synechocystis* and subsequent analysis of the resulting phenotypes by a variety of techniques, including flash-induced fluorescence to monitor the integrity of the electron transfer reaction from H_2O to Y_Z^+ (Boerner et al., 1992; Diner & Nixon, 1992; Nixon & Diner, 1992; Nixon et al., 1992; Chu et al., 1994a,b). Some clearly important results have been obtained by the mutant approach, such as the identification of residues that, when mutated, result in complete inhibition of O_2 evolution. Asp170 and His332 on the D1 RC protein are examples (Boerner et al., 1992; Nixon & Diner, 1992). Nevertheless, some of the results obtained by the genetic approach have been difficult to explain (Debus, 1992; Chu et al., 1994a,b).

† The National Renewable Energy Laboratory is operated by the Midwest Research Institute for the U.S. Department of Energy under Contract DE-AC36-83CH10093. This work was supported by the Energy Biosciences Division, Office of Basic Energy Sciences, U.S. Department of Energy (M.S.). M.L.G. and T.W.L. are Associated Western Universities Research Associates at the NREL.

* To whom correspondence should be addressed. Telephone: (303) 384-6279. Fax: (303) 384-6150. E-mail: seibertm@tcplink.nrel.gov.

⊗ Abstract published in *Advance ACS Abstracts,* January 15, 1996.

[1] Abbreviations: Chl, chlorophyll; cyt b_{559}, cytochrome b_{559}; DCIP, 2,6-dichlorophenolindophenol; DCMU, 3-(3,4-dichlorophenyl)-1,1-dimethylurea; DEPC, diethyl pyrocarbonate; DPC, 1,5-diphenylcarbazide; K_i, dissociation constant of the enzyme−inhibitor complex; K_m, Michaelis−Menten constant for an enzymatic reaction; k_n, rate constant of a particular step of a reaction; MES, 2-(*N*-morpholino)ethanesulfonic acid; P_{680}, reaction center primary electron donor in photosystem II; Pheo, pheophytin; PSII, photosystem II; Tris, tris(hydroxymethyl)-aminomethane; V_{max}, maximum initial rate of an enzymatic reaction; Y_Z, tyrosine 161 on the D1 protein in spinach, the first electron donor to P_{680}^+ in PSII; Y_D, tyrosine 160 on the D2 protein in spinach, an alternative donor to P_{680}^+ in PSII.

0006-2960/96/0435-1820$12.00/0

The other approach for studying Mn-binding ligands has involved biochemical alterations, including chemical modification of amino acid residues and/or partial proteolytic digestion of the D1 and D2 proteins in Mn-depleted PSII membranes (Tamura et al., 1989; Seibert et al., 1989; Preston & Seibert, 1989, 1991a,b). These alterations prevent exogenous Mn from binding to Tris-treated membranes and affect the ability of added Mn to inhibit DPC electron donation to PSII. Hydroxylamine and Tris treatment (Yamashita & Butler, 1968; Cheniae & Martin, 1970) of PSII membranes removes the functional Mn cluster (Klimov et al., 1982), and both Y_Z^+ and Y_D^+ become accessible to exogenous donors (Babcock & Sauer, 1975). Under these conditions, either diphenylcarbazide (DPC) or Mn^{2+}, when added separately, can donate electrons at two sites in PSII, as monitored by titrating the rates of DCIP photoreduction (Blubaugh & Cheniae, 1990; Ghirardi & Seibert, 1992). One of the sites is a high-affinity site through which Y_Z^+ is reduced (Hoganson et al., 1989; Blubaugh & Cheniae, 1990; Miller & Brudvig, 1990; Nixon & Diner, 1992), and the other is a low-affinity site where Y_D^+ is proposed to be reduced (Blubaugh et al., 1991). Diphenylcarbazide at 200 μM donates at equal rates to both sites, but addition of 10 μM $MnCl_2$ noncompetitively inhibits DPC photooxidation by Y_Z only at the high-affinity PSII site (Preston & Seibert, 1991a; Ghirardi & Seibert, 1992). The result is a 50% decrease in the rate of DCIP photoreduction.

Since the "DPC inhibition assay" requires prior removal of the functional Mn cluster from PSII membranes, oxygen evolution function is lost. While the assay detects a high-affinity Mn site, it has been unclear how this site is related to the binding of the active Mn cluster. Besides the possibility that the assay is not detecting Mn sites of physiological importance, the occurrence of back dark-reactions between Mn^{3+} and DPC or $DCIPH_2$ has been invoked as a potential cause for interference with the assay (Hoganson et al., 1989). This last issue was addressed by Preston and Seibert (1991a), who demonstrated that these dark reactions were slow.

In the present work, we have tried to answer experimentally some of the remaining questions concerning the use of the DPC inhibition assay as a probe for Mn binding in PSII. More specifically, we address the question of whether the estimated K_i for Mn inhibition reflects the binding of Mn^{3+}, or Mn^{2+}, to the membranes, by investigating whether Mn^{2+} photooxidation is required for inhibition of DPC photooxidation by Y_Z^+, and whether it in fact occurs under the assay conditions, as suggested by our previous data (Preston & Seibert, 1991b). The results of this investigation provide evidence that, although Mn^{2+} photooxidation by PSII does occur in the presence of bound DPC, it is not necessarily required for inhibition of DPC photooxidation by Y_Z^+. Based on our previous observation that the high-affinity Mn-binding site detected by the DPC inhibition assay can be deconvoluted into four independent components (Preston & Seibert, 1991a,b), we suggest that each component binds a Mn ion, and that only one of the bound Mn is photooxidized by Y_Z^+ in the presence or absence of DPC.

MATERIALS AND METHODS

Spinach was obtained locally, and PSII-enriched appressed membrane fragments were prepared as before (Preston & Seibert, 1991a). Chlorophyll concentrations and Chl *a*/*b* ratios were determined in 80% acetone, according to the method of Arnon (1949). The functional manganese cluster and the three extrinsic polypeptides (17, 23, and 33 kDa) required for photosynthetic oxygen evolution were removed by incubating the PSII membranes (500 μg of Chl/mL) in 1 M Tris-HCl, pH 9.4, containing 0.4 M sucrose for 30 min at 5 °C under room light (Preston & Seibert, 1991a). This method typically leaves a small amount of Mn attached to the membranes, since the rate of DCIP photoreduction in the absence of added donors is not zero. The membranes were then collected by centrifugation at 32000*g* for 10 min, washed 3 times in 20 mM MES, pH 6.5, containing 0.4 M sucrose, 15 mM NaCl, and 5 mM $MgCl_2$ (buffer A), and stored at −80 °C in small vials until use.

DCIP photoreduction was measured at 600 nm using an Aminco DW2a spectrophotometer in the split-beam mode and outfitted with red (630 nm cut-on Schott RG630 filter) actinic side illumination (Preston & Seibert, 1991a). The photomultiplier was protected from the actinic excitation with a 600 nm narrow band-pass filter (Melles Griot 03FIV045). Data collection and processing of the spectrophotometer output were performed using Data Translation Global Lab^R software and a DT2839 A/D board mounted in an ALR 486 PC. The assay medium contained 50 mM MES, pH 6.5, 20 mM NaCl, 0.8 M sucrose, 30−75 μM DCIP, and 5 μg of Chl/mL of Tris-treated PSII membranes. DPC was added to a final concentration of 200 μM, unless otherwise specified in the text. Each DCIP photoreduction rate reported was an average of 2−3 experiments. The residual rate obtained in the absence of an added donor, which was less than 5% of the rate of electron donation measured in the presence of 200 μM DPC, was subtracted prior to determination of the initial slopes. Manganese, zinc, and cobalt were added as divalent chloride salts. Curve-fitting, including the data in the Dixon Plots and kinetic modeling, employed Grafit 3.0 software (Leatherbarrow, 1992), as described in the Appendix.

The decay of the flash-induced variable fluorescence yield was measured with a home-built instrument (Kramer & Crofts, 1990; Nishio and Lane, personal communication). Saturating actinic light was provied by an EG&G FX201 Xenon flash lamp (3 μs HWHM) filtered through a Corion LS-650 band-pass filter. Weak monitoring flashes, provided by an array of Hewlett-Packard HLMA-CHOO light-emitting diodes (LED, 621 nm emission, 100 Hz flash rate), were applied during the experiment to measure the flash-induced fluorescence yield, measured as $(F - F_0)/F_0$ (Chu et al., 1995). The optimal nonactinic intensity and flash rate of the monitoring flashes were determined by observing a lack of change in the fluorescence yield induced by the LED array alone for up to 20 s. Fluorescence emission was detected by a Hamamatsu S2744-03 PIN silicone photodiode protected by a Corion RG-715 cut-on filter. The photodiode signal was amplified using a home-built circuit. The detection system was gated for the first 100 μs to protect the detector from saturation by the actinic flash. Data were collected using a Data Translation DT2839 A/D board mounted in an ALR 486 PC and Global Lab data acquisition software. Analysis of the data began 2−3 ms after the actinic flash. F_0 was obtained by starting the LEDs 0.5 s prior to an actinic flash and measuring the resulting fluorescence yield.

Samples used for fluorescence measurements were dark-adapted, Tris-treated PSII membranes from spinach diluted in 1 mL of buffer A to a final Chl concentration of 27 μg/mL. DCMU (50 μM) was added to block electron transfer from Q_A^- to Q_B. Addition of 0.3 mM potassium ferricyanide and 0.3 mM *p*-benzoquinone to preoxidize the reducing side of PSII (Nixon & Diner, 1992; Chu et al., 1994a,b) did not affect the variable fluorescence yield detected after the flash (not shown). Thus, these acceptors were not used in our experiments. The samples were placed in a 4 mm × 10 mm cuvette and excited at the 10 mm face. Fluorescence emission was detected at a 90° angle from the actinic and probe flashes.

RESULTS

Effect of Zn, Co, and Mn on DPC Photooxidation by PSII. A number of heavy metals, such as zinc, cadmium, cobalt, nickel, and mercury, interact with PSII and inhibit its activity. The inhibitory mechanism of these metals is not known, but has been the subject of previous research. Zinc effects have been attributed to its interaction at two sites (Rashid et al., 1991). Micromolar concentrations of zinc act on the oxidizing side of PSII, while millimolar concentrations of the metal act at a secondary site on the reducing side (Mohanty et al., 1989; Rashid et al., 1991). The inhibition on the oxidizing side is thought to result from displacement of the functional manganese cluster, since addition of micromolar concentrations of $ZnCl_2$ to PSII membranes promotes the release of Mn^{2+}, concomitant with loss of O_2 evolution and electron transfer capacity (Rashid et al., 1991). Cobalt also inhibits the oxidizing side of PSII and binds with high affinity to a site physically close to Y_Z (Tripaty et al., 1983; Hoganson et al., 1991).

The evidence for interactions between zinc and cobalt with the oxidizing side of PSII makes the two metals good candidates for assessing effects on manganese inhibition of DPC photooxidation. However, there are reports in the literature suggesting that Zn^{2+} (but not Co^{2+}) may form complexes with DPC (Hoganson et al., 1991). For these reasons, we chose to examine interactions of Mn^{2+} with both Zn^{2+} and Co^{2+} as potential inhibitors of DPC photooxidation.

In order to interpret the data presented below, it is important first to demonstrate that neither Zn^{2+} nor Co^{2+} acts as an electron donor to PSII under our experimental conditions. To do this, we added $ZnCl_2$ and $CoCl_2$ separately to Tris-treated PSII membranes in the absence of other electron donors. Figure 1 shows that neither cation photoreduces DCIP when present at a concentration of 100 μM or higher (not shown). In contrast, even at low concentration (10 μM), $MnCl_2$ is able to donate electrons to PSII.

Figure 2A shows the effect of adding $MnCl_2$, $ZnCl_2$, and $CoCl_2$ separately to PSII membranes in the presence of 200 μM DPC. As previously reported, addition of up to 10 μM $MnCl_2$ inhibits about 50% of the rate of DCIP photoreduction by 200 μM DPC, due to noncompetitive interactions between Mn and DPC at the high-affinity site (Preston & Seibert, 1991a,b; Ghirardi & Seibert, 1992). Higher concentrations of added $MnCl_2$ result in an increase in the rate of DCIP photoreduction by PSII, due to binding and photooxidation of Mn^{2+} at the low-affinity site in PSII. Figure 2A shows that both $ZnCl_2$ and $CoCl_2$ are also able to inhibit DPC photooxidation by PSII. The Dixon plot (1/initial rate vs

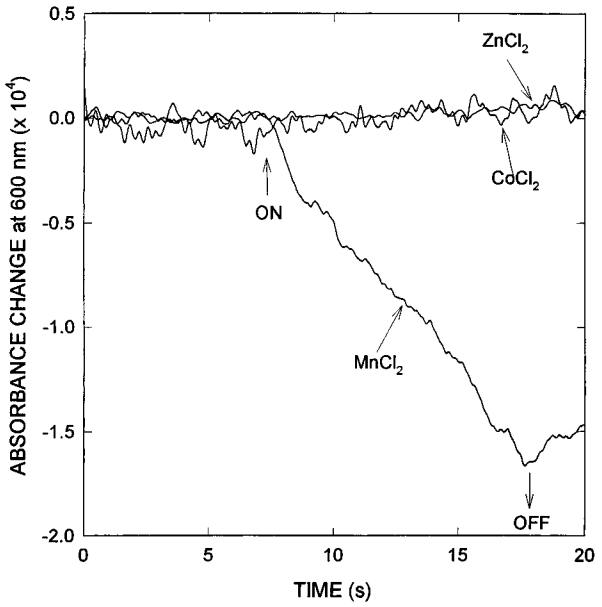

FIGURE 1: Light-induced DCIP reduction by 10 μM $MnCl_2$, 100 μM $ZnCl_2$, or 100 μM $CoCl_2$. Absorbance changes due to DCIP photoreduction were monitored at 600 nm. The curves have been corrected for the residual absorbance changes observed in the absence of added divalent cations. Arrows indicate when the actinic light was turned on and off.

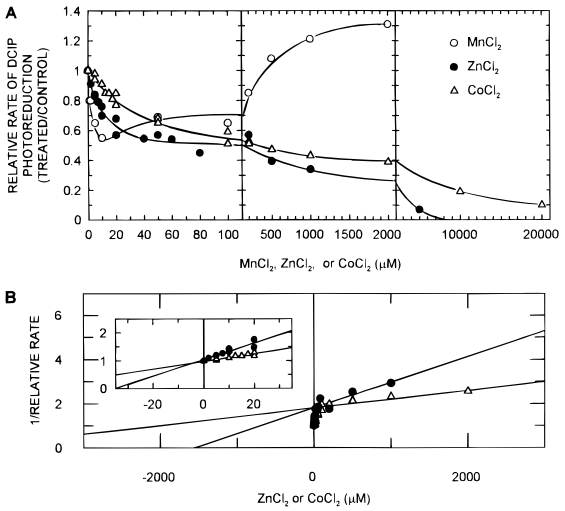

FIGURE 2: Effect of different divalent cations on the rate of DPC photooxidation. (A) Relative rate of DPC photooxidation, expressed as the initial rate of DCIP photoreduction in the presence of 200 μM DPC as a function of different concentrations of added $MnCl_2$ (○), $ZnCl_2$ (●), or $CoCl_2$ (△). Rates measured in the absence of inhibitors were 89, 152, and 117 μmol of DCIP·(mg of Chl)$^{-1}$·h^{-1} for the $MnCl_2$, $ZnCl_2$, and $CoCl_2$ experiments, respectively. (B) Plot of the inverse of the relative initial rate of DCIP photoreduction by DPC versus the concentration of added $ZnCl_2$ (●) or $CoCl_2$ (△).

inhibitor concentration; Segel, 1993) shown in Figure 2B demonstrates that inhibition of DPC electron donation by either $ZnCl_2$ or $CoCl_2$ is biphasic. The high-affinity component is responsible for inhibiting about 50% of the DPC electron donation rate and has a K_i in the micromolar range for both ions (the high-affinity components are expanded in the inset of Figure 2B). A low-affinity component with a K_i in the millimolar range (Figure 2B) inhibits the remaining 50% of the electron donation rate in both cases.

To determine whether Mn^{2+}, Zn^{2+}, and Co^{2+} share high-affinity binding sites in PSII, we repeated the metal titration of DPC electron donation in the absence or presence of either

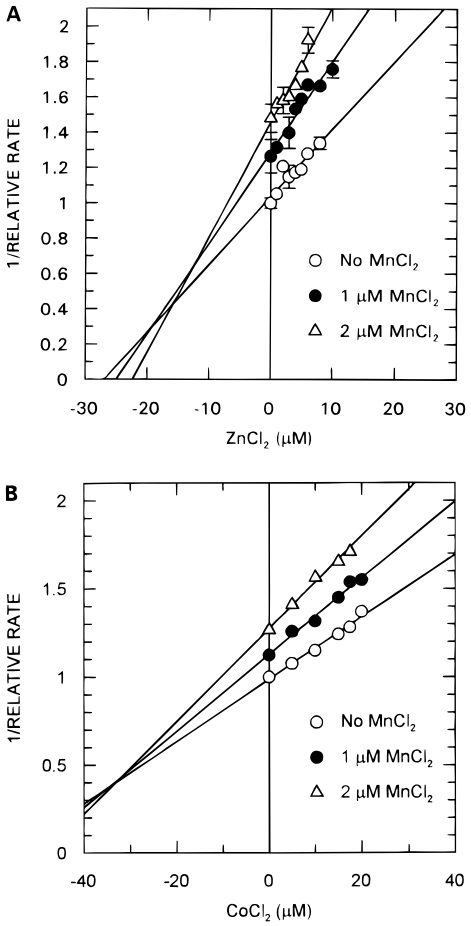

FIGURE 3: Interaction between Zn^{2+}, Co^{2+}, and Mn^{2+} in the inhibition of DPC photooxidation. Relative rates of DCIP photoreduction by 200 μM DPC as a function of added $ZnCl_2$ or $CoCl_2$ were measured either in the absence of $MnCl_2$ (○) or in the presence of 1 μM (●) or 2 μM (△) $MnCl_2$. Rates measured in the absence of inhibitors were 119 and 195 μmol of DCIP·(mg of Chl)$^{-1}$·h^{-1}, respectively, for the $ZnCl_2$ and the $CoCl_2$ experiments. (A) Plot of the inverse of the relative rate of DCIP photoreduction as a function of $ZnCl_2$ concentration. Error bars (standard deviations) were added to a few representative points in order to indicate the precision of our experiments. Linear regression analysis shows that the three lines intercept above the abscissa at approximately $x = -18$, which indicates a nonmutually exclusive interaction between Zn^{2+} and Mn^{2+}, with an apparent K_i of 18 μM for Zn^{2+}. (B) Plot of the inverse of the relative rate of DCIP photoreduction as a function of $CoCl_2$ concentration. Linear regression analysis shows that the three lines intercept above the abscissa at approximately $x = -33$, which indicates a nonmutually exclusive interaction between Co^{2+} and Mn^{2+}, with an apparent K_i of 33 μM for Co^{2+}.

1 μM $MnCl_2$ or 2 μM $MnCl_2$. The nature of the interaction between the two inhibitors (mutually exclusive vs nonmutually exclusive) was determined from the Dixon plots (1/initial rate vs inhibitor concentration) in Figure 3A,B. In both cases, the curves are not parallel but intercept to the left of the ordinate, which indicates a nonmutually exclusive interaction (Segel, 1993). This means that the binding of one inhibitor does not entirely prevent the binding of the second inhibitor, suggesting that they may share some, but not all, binding sites. The observation that the intercepts are located above the *x*-axis could be due to (a) the fact that the low concentration of metal ions used in the experiments affects only the high-affinity component of the DPC-mediated DCIP reduction reaction, and/or (b) the existence of cooperative inhibitor binding, i.e., binding of one of the metals facilitates the binding of the other metal at a different site (Segel, 1993). The point at which the curves intercept is an estimate of the K_i for $ZnCl_2$ (Figure 3A) and $CoCl_2$ (Figure 3B) at the high-affinity site. The estimated values are about 18 μM for $ZnCl_2$ and 33 μM for $CoCl_2$.

In a nonmutually exclusive interaction, the binding of one inhibitor can still partially affect the binding of the second inhibitor. This is usually due to allosteric effects associated with the binding of the two inhibitors at different sites (Segel, 1993). On the other hand, we have previously demonstrated that the high-affinity, Mn-binding site associated with inhibition of DPC photooxidation can be deconvoluted into at least four independent components, corresponding to four distinct amino acid residues (Preston & Seibert, 1991b). In this situation, the effects of the metal inhibitor on the binding of Mn could be attributed to the presence of two types of binding components for Mn^{2+}. Some of the components could be common to Mn^{2+} and to the other two metal ions (i.e., mutually exclusive), and other components could be specific for Mn^{2+} only (i.e., nonmutually exclusive). However, the results reported above on the interaction between Mn^{2+}, Zn^{2+}, and Co^{2+} do not allow us to determine conclusively whether the three ions share some of the same binding components or not.

Effect of Added DPC, Zn, Co, and Mn on the Decay of the Flash-Induced Variable Fluorescence Yield in Tris-Treated PSII Membranes at a High-Affinity Site. Charge recombination between Y_Z^+ and Q_A^- in Tris-treated samples has a half-life of 15−100 ms (Dekker et al., 1984; Metz et al., 1989; Nixon & Diner, 1992; Boerner et al., 1992; Chu et al., 1994a,b). It can be monitored by the decay of the fluorescence yield detected by weak nonactinic probes following a single saturating flash in DCMU-treated samples (Joliot & Joliot, 1984; Debus, 1992; Diner & Nixon, 1992). The addition of electron donors to Y_Z^+, such as DPC or Mn^{2+}, prevents charge recombination [however, see Miller and Brudvig (1990)] and results in no observable decay in the fluorescence level after a flash, due to the accumulation of Q_A^- on the reducing side of PSII (Nixon & Diner, 1992). Figure 4A shows the decay of the variable fluorescence after addition of, respectively, 0, 40 μM, 200 μM, and 1 mM DPC to Tris-treated spinach PSII membranes in the presence of 50 μM DCMU. In the absence of DPC, the initial fluorescence yield (F_M) decays to an intermediate F_{final} level with a half-life of about 30 ms. F_{final} is typically 20−25% of F_{max}, suggesting that Q_A^- does not recombine with Y_Z^+ in a significant percentage of PSII centers. This phenomenon has been previously addressed by Metz et al. (1989). They suggested that 20−25% of the PSII centers in the charge-separated state $P_{680}^+Q_A^-$ may have lost Y_Z^+ through reduction by a more distant donor, or may not have generated Y_Z^+ in all centers due to competition with parallel pathways for electron donation to P_{680}^+. In either situation, fast charge recombination with Q_A^- is prevented, and the fluorescence level stays above F_0. Some of the nondecaying fluorescence yield may also be attributed to small amounts of exogenous Mn^{2+} in the preparation which may act as an electron donor to Y_Z^+. Higher concentrations of added DPC increase F_{final}, indicating accumulation of Q_A^- due to increasing electron donation to Y_Z^+.

Figure 4B shows the decay of the flash-induced fluorescence yield, upon addition of either 10 μM $MnCl_2$ (a donor to PSII) or 100 μM $ZnCl_2$ or 100 μM $CoCl_2$ (neither photooxidized by PSII) to DCMU-treated membranes. Fig-

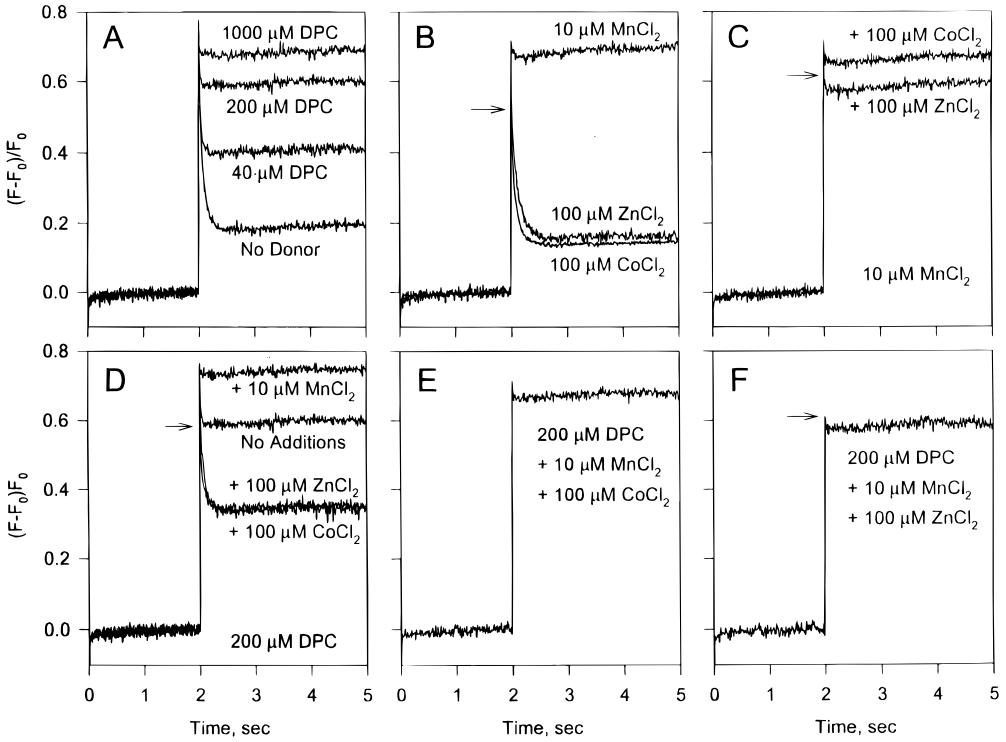

FIGURE 4: Effect of addition of different combinations of electron donors and divalent cations on the decay of the flash-induced fluorescence yield. Each sample contained 27 μg of Chl/mL of Tris-treated PSII membranes and 50 μM DCMU. Other experimental conditions are described in the text. (A) Measurements done in the absence of electron donors and in the presence of, respectively, 40, 200, or 1000 μM DPC; (B) addition of either 10 μM $MnCl_2$, 100 μM $ZnCl_2$, or 100 μM $CoCl_2$; (C) addition of mixtures of 10 μM $MnCl_2$ with either $ZnCl_2$ or $CoCl_2$; (D) addition of 200 μM DPC with either $MnCl_2$, $ZnCl_2$, or $CoCl_2$; (E) addition of a mixture of DPC, $MnCl_2$, and $CoCl_2$; (F) addition of a mixture of DPC, $MnCl_2$, and $ZnCl_2$. The addition of $ZnCl_2$ alone or in combination with either DPC or $MnCl_2$ causes a small but measurable quenching of the F_{max}, as indicated by the arrows in panels B, C, D, and F.

ure 4C shows the effect of adding a mixture of $MnCl_2$ with either of the two salts to DCMU-treated membranes. It is clear that neither $ZnCl_2$ nor $CoCl_2$ donates electrons to Y_Z^+ significantly at this concentration (see also Figure 1), while $MnCl_2$ effectively blocks charge recombination by re-reducing Y_Z^+. We have reported a K_m of about 1.5 μM for $MnCl_2$ photooxidation at the high-affinity site in Tris-treated PSII membranes (Ghirardi & Seibert, 1992; see also Appendix), which is consistent with the complete elimination of fluorescence decay by 10 μM $MnCl_2$. Addition of either 100 μM $ZnCl_2$ or 100 μM $CoCl_2$ to 10 μM $MnCl_2$ does not have a significant effect on the extent of Mn^{2+} photooxidation by PSII. This indicates that neither ion inhibits single-turnover Mn^{2+} photooxidation by PSII at this particular concentration.

In order to determine whether Mn inhibition of DPC photooxidation at a high-affinity site is accompanied by at least one photooxidation of Mn^{2+}, we monitored the decay in the flash-induced fluorescence yield upon addition of 200 μM DPC to 10 μM $MnCl_2$. As seen above, both donors, when added separately at these concentrations, either partially or totally prevent charge recombination in PSII. Figure 4D shows the decay of the flash-induced fluorescence yield in the presence of DPC; DPC and $MnCl_2$; DPC and $ZnCl_2$; and DPC and $CoCl_2$. Figure 4E,F shows the effect of mixtures of DPC and a combination of two of the three salts. When both DPC and $MnCl_2$ are present, reduction of Y_Z^+ does occur after a single flash. In contrast to the lack of effect of $ZnCl_2$ and $CoCl_2$ on the single-turnover Mn^{2+} photooxidation by PSII (see Figure 4C), addition of 100 μM $ZnCl_2$ or $CoCl_2$ partially blocks reduction of Y_Z^+ by DPC (Figure 4D). The differential effect of $ZnCl_2$ and $CoCl_2$ on electron donation by DPC (Figure 4D) and Mn^{2+} (Figure 4C) to PSII was used to identify the electron-donating species in the DPC plus $MnCl_2$ mixture. When either $ZnCl_2$ or $CoCl_2$ is added to the DPC−$MnCl_2$ mixture, the fluorescence yield does not decay, which indicates that the observed single electron donation to Y_Z^+ in the mixture must thus be mediated by Mn^{2+}, not DPC.

Modeling Mn Inhibition of DCIP Photoreduction in the Presence of 200 μM DPC. The *flash* results described above clearly show that at least one Mn^{2+} photooxidation per PSII center occurs in the presence of bound DPC, and that it is not inhibited by $ZnCl_2$ or $CoCl_2$. This suggests that the high-affinity site at which Mn^{2+} photooxidation occurs is not shared with the other metal ions. This observation is consistent with the results in Figure 3A,B, which show that Mn may share some but not all binding sites with Zn or Co in the presence of DPC. However, the above experiments do not provide any indication of the amount of *steady-state* Mn^{2+} photooxidation occurring in the presence of DPC. We have previously estimated that only about one Mn^{3+} is photoproduced on average per center per second in the presence of 200 μM DPC and 10 μM $MnCl_2$ (Preston & Seibert, 1991a). In contrast, the estimated rate of Mn^{2+} photooxidation (at 10 μM) in the absence of DPC has been reported to be much higher (5−20 Mn^{3+} photoproduced per RC per second; Preston & Seibert, 1991a). Metal analysis revealed that only 1 Mn atom per RC is strongly bound to PSII membranes in the absence of DPC, but 3−4 Mn atoms per RC are detected when 200 μM DPC is added (Preston & Seibert, 1991b). This suggests that as few as one of possibly four Mn atoms bound in the presence of DPC is photooxidizable by PSII.

In order to determine the extent of steady-state Mn^{2+} photooxidation that occurs in the presence of bound DPC, we modeled the titration of DPC inhibition by $MnCl_2$ in the following situations: (a) steady-state Mn^{2+} photooxidation is inhibited in the presence of DPC (which does not exclude the possibility that a single photooxidation of Mn occurs under these conditions, as seen previously); and (b) no inhibition of steady-state Mn^{2+} photooxidation by DPC occurs (see Appendix for a quantitative description of both DPC and Mn^{2+} photooxidation by PSII).

Model a is represented by eq 1. In this case, DPC and Mn inhibit each other noncompetitively at both the low- and high-affinity sites, and binding of both Mn^{2+} and DPC to

$$v = \frac{V_1}{(1 + K_1/d)(1 + m/K_{i3})} + \frac{V_2}{(1 + K_2/d)(1 + m/K_{i4})} + \frac{V_3}{(1 + K_3/m)(1 + d/K_{i1})} + \frac{V_4}{(1 + K_4/m)(1 + d/K_{i2})} \quad (1)$$

sites on the same center prevents steady-state photooxidation of the other donor. The rate of DCIP photoreduction measured in the presence of different amounts of DPC and $MnCl_2$ is represented by the variable v in eqs 1 and 2. K_{i1} and K_{i2} represent the inhibition constants associated with DPC inhibition of Mn^{2+} photooxidation at, respectively, the high- and low-affinity sites. K_{i3} and K_{i4} represent the inhibition constants associated with Mn^{2+} inhibition of DPC photooxidation at the high- and low-affinity PSII sites.

Model b is represented by eq 2, which shows that DPC photooxidation is noncompetitively inhibited by Mn at both the high- and low-affinity sites. Mn^{2+} photooxidation, however, is not affected by the presence of DPC.

$$v = \frac{V_1}{(1 + K_1/d)(1 + m/K_{i3})} + \frac{V_2}{(1 + K_2/d)(1 + m/K_{i4})} + \frac{V_3}{1 + K_3/m} + \frac{V_4}{1 + K_4/m} \quad (2)$$

The other kinetic parameters for Mn and DPC required by eqs 1 and 2 were defined and determined as described in the Appendix. The following additional assumption was made: the K_is associated with binding of DPC or Mn to each site are to the first approximation equal to the corresponding K_ms for DPC or Mn^{2+} photooxidation.

Figure 5 shows the relative rate of DCIP photoreduction by 200 μM DPC upon addition of an increasing concentration of $MnCl_2$. As shown in Figure 2A, the maximum inhibition, corresponding to a decrease in the relative rate of DCIP reduction to about 0.5 under our experimental conditions, is achieved with 10 μM $MnCl_2$. The addition of higher concentrations of $MnCl_2$ results in an increase in the rate of DCIP reduction by PSII, due to photooxidation of Mn^{2+} in centers containing a low-affinity PSII site that does not bind DPC under our experimental conditions (Ghirardi & Seibert, 1992). The two curves shown in Figure 5 correspond to fits of models a and b. It is clear from Figure 5 that DPC must inhibit steady-state Mn^{2+} photooxidation at the high-affinity site (Y_Z).

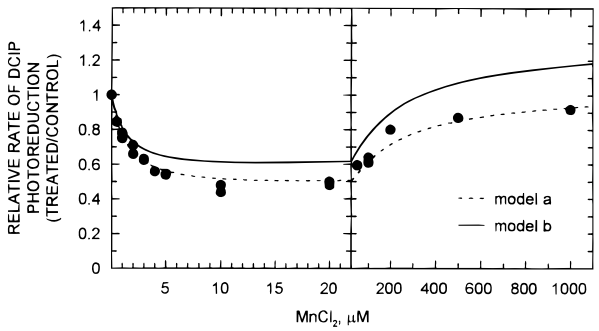

FIGURE 5: Modeling of the inhibition of DPC-mediated DCIP photoreduction by increasing concentrations of $MnCl_2$. The closed circles (●) represent experimental data (obtained under the same experimental conditions described for Figure 2). The lines represent the kinetic models a and b described in the text. The rate of DCIP photoreduction measured in the absence of added $MnCl_2$ was 89 μmol of DCIP·(mg of Chl)$^{-1}$·h^{-1}.

DISCUSSION

The nature of the amino acid residues that bind manganese on the oxidizing side of PSII has been an area of intensive research in the past and has been investigated by a variety of different approaches as described in the introduction. We have employed the DPC inhibition assay to identify some of the Mn-binding ligands in PSII (Seibert et al., 1989; Preston & Seibert, 1989, 1990, 1991a,b; Ghirardi & Seibert, 1992, 1995). In the current study, we address the question of whether the Mn-binding components detected by the assay are related to ligands that bind Mn of physiological importance to O_2 evolution.

As we have shown above, there is little if any steadyhstate Mn^{2+} photooxidation occurring in the presence of bound DPC, and Mn^{2+} photooxidation is not necessarily a requirement for inhibition of DPC donation at high affinity to PSII. This suggests that the K_i for Mn inhibition of DPC photooxidation is not significantly influenced by the binding of Mn^{3+} to the membrane. However, comparing steady-state and single-turnover flash data, we also demonstrate that, although Mn^{2+} photooxidation is not necessarily required for inhibition of DPC electron donation to Y_Z^+, at least one Mn bound to PSII is photooxidized in the presence of DPC after a saturating flash. Given that three to four Mn are bound to PSII in the presence of DPC (Preston & Seibert, 1991b), we conclude that the DPC inhibition assay detects two types of amino acid components that bind Mn in PSII: (a) one that is nonspecific for Mn, i.e., it also binds either Zn^{2+} or Co^{2+}; and (b) a second type of component that specifically binds Mn^{2+} and allows it to be photooxidized at least once, even in the presence of DPC.

There is ample evidence in the literature for the nonequivalency of Mn-binding sites on the oxidizing side of PSII (Dismukes, 1986). Two of the four Mn ions from the Mn cluster can be released easily from the membranes by a number of chemical treatments (Cheniae, 1980; Kuwabara & Murata, 1983; Miller & Cox, 1983; Ono & Inoue, 1983; Packham & Barber, 1984). Observations of steady-state Q_A or Pheo photoreduction in Mn-depleted membranes are observed upon rebinding of either four Mn per RC or, alternatively, by addition of only two Mn plus two other divalent cations per RC under nonphotoactivating conditions (Klimov et al., 1982). These results were the basis for the suggestion that some of the Mn required for O_2 evolution may function structurally but not catalytically on the oxidizing side of PSII (Dismukes, 1986). The structural Mn sites may be "competitive" with other divalent cations in the absence of a functional cluster.

Photoactivation experiments also support the idea of nonequivalency of Mn-binding sites. The photoligation of the first Mn to PSII requires photooxidation of Mn^{2+} to Mn^{3+} (Tamura & Cheniae, 1987; Ananyev et al., 1988), and may involve Asp170 on D1 (Boerner et al., 1992; Nixon & Diner, 1992; Whitelegge et al., 1995). The second Mn^{2+} binds to PSII and forms a relatively more stable Mn^{3+}/Mn^{3+} complex after a second photoact. DEPC treatment of NH_2OH-treated membranes indicates that a histidine residue may ligate the second Mn during photoactivation (Blubaugh & Cheniae, 1992). The ligation of the two final Mn occurs in the dark, and generates the stable tetrameric manganese cluster (Tamura & Cheniae, 1987).

We have employed both steady-state and flash techniques to study Mn binding to Tris-treated PSII membranes. Although our steady-state work detects four high-affinity Mn-binding components, the flash data indicate that only one of the components binds a photooxidizable Mn. This demonstrates that the Mn-specific binding site detected by the DPC inhibition assay is of physiological importance to photosynthesis. We suggest that this component is Asp170 on D1, the proposed ligand to the first Mn bound in the photoactivation process. Other Mn-binding amino acid ligands detected by this assay, such as His337 on D1 (Preston & Seibert, 1990, 1991b), may be the components that are not specific for Mn. Recent experiments from Dr. R. Debus' laboratory (Chu et al., 1995) also indicate that His337 on D1 is a PSII Mn ligand. Since we have the capability of "isolating" each of four amino acid components of the high-affinity Mn site by means of partial proteolysis and chemical modification of PSII membranes (Preston & Seibert, 1991a,b), we will use this capability to further examine the nonequivalency of the four components with respect to Mn^{2+} photooxidation and binding of cations other than manganese.

ACKNOWLEDGMENT

We appreciate the helpful discussion and suggestions of Drs. R. Debus, C. Dismukes, and T. Wydrzynski. We also thank Dr. G. Cheniae for reviewing an early version of the manuscript. Technical information on the flash fluorometer was kindly provided to us by Drs. D. Kramer and J. Nishio and by R. Lane.

APPENDIX

In the absence of the manganese cluster, PSII, following an initial photoact, can be re-reduced by a number of exogenous reductants, such as DPC or Mn^{2+}. Equation 3

$$Mn^{2+} + [PSII] \underset{k_2}{\overset{k_1}{\rightleftharpoons}} [Mn^{2+}\cdot PSII] \xrightarrow{h\nu} [Mn^{2+}\cdot PSII^{+}] \xrightarrow{k_3} [Mn^{3+}\cdot PSII] \underset{k_5}{\overset{k_4}{\rightleftharpoons}} Mn^{3+} + [PSII] \quad (3)$$

describes the photooxidation of exogenously-added Mn^{2+} at the high-affinity site in Tris-treated PSII membranes. The reaction, as described, takes place under saturating light conditions and in the presence of saturating amounts of the electron acceptor dichlorophenolindophenol (DCIP). The Michaelis−Menten constant (K_m) for Mn^{2+} photooxidation in the above equation depends on the values of (a) the dissociation constant k_2/k_1 for Mn^{2+} binding to the membranes, (b) the rate constant k_3 for the reduction of light-generated Y_Z^+ by Mn^{2+}, and (c) the dissociation constant k_4/k_5 of the resulting Mn^{3+} at the same site. The kinetic parameter V_{max} (defined as k_3[PSII]) describes the maximum turnover rate of PSII, when the concentration of Mn^{2+} is saturating. Photooxidation of DPC can be described by a similar equation, with corresponding rate constants. The rates of DPC or Mn^{2+} photooxidation are determined experimentally from the initial rates of DCIP photoreduction.

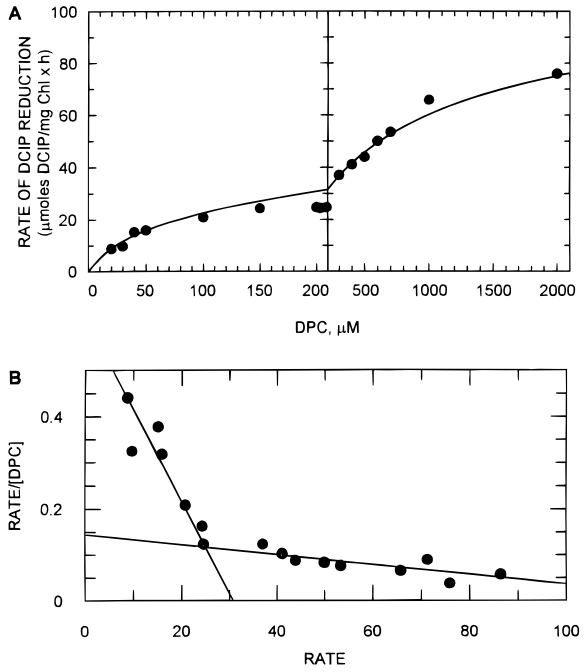

FIGURE 6: (A) Rate of DPC photooxidation by PSII, expressed as the initial rate of DCIP photoreduction, as a function of the concentration of added DPC. The experimental data were fitted to a two-enzyme Michaelis−Menten equation (solid line), using the kinetic parameters obtained below. (B) Eadie−Hofstee plot of the DPC titration experiment in (A). The data points yield two straight lines defining two independent photooxidation sites for DPC. Initial estimates for V_{max} and K_m at each site were obtained, respectively, from the *x*-intercepts and −1/slope for each line. Final estimates were determined as described under Materials and Methods and are given in the text.

The initial rate of DCIP reduction as a function of the concentration of added Mn^{2+} (υ_{Mn}) or DPC (υ_{DPC}) at both high- and low-affinity sites can be derived from eq 3 by using a two-enzyme Michaelis−Menten model (Segel, 1993). Equation 4 is based on the observation that each donor, when added separately, is photooxidized at two independent sites in PSII membranes: a high-affinity site ($V_{max} = V_1$, $K_m = K_1$ for DPC; and $V_{max} = V_3$, $K_m = K_3$ for Mn^{2+}) and a low-affinity site ($V_{max} = V_2$, $K_m = K_2$ for DPC; $V_{max} = V_4$, $K_m = K_4$ for Mn^{2+}). The variables *d* and *m* represent the concentrations of added DPC and $MnCl_2$, respectively.

$$\upsilon_{DPC} = \frac{V_1}{1 + K_1/d} + \frac{V_2}{1 + K_2/d}; \; \upsilon_{Mn} = \frac{V_3}{1 + K_3/m} + \frac{V_4}{1 + K_4/m} \quad (4)$$

The modeling of the $MnCl_2$ titration of DPC inhibition requires estimated values for V_{max} and K_m for both DPC and manganese at the high- and low-affinity sites in PSII (see eqs 1 and 2). Kinetic parameters for Mn^{2+} and DPC photooxidation by Tris-treated PSII membranes were deter-

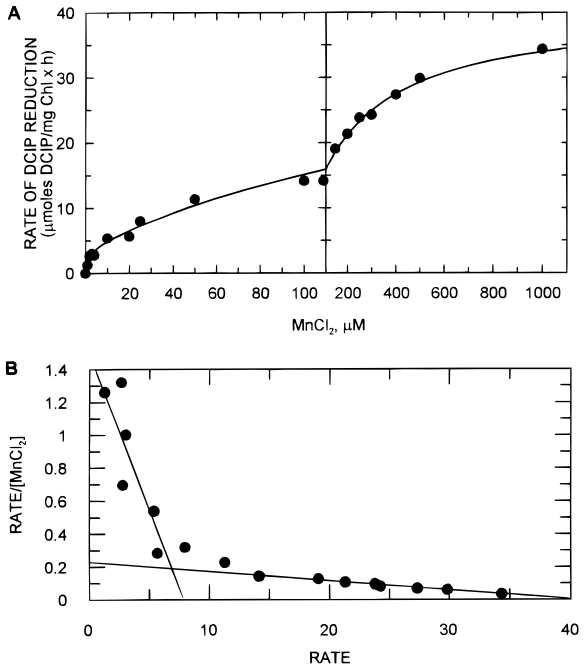

FIGURE 7: (A) Rate of manganese photooxidation by PSII, expressed as the initial rate of DCIP photoreduction, as a function of the concentration of added $MnCl_2$. The experimental data were fitted to a two-enzyme Michaelis−Menten equation (solid line) using the kinetic parameters obtained below. (B) Eadie−Hofstee plot of the $MnCl_2$ titration experiment in (A). The data points yield two straight lines defining two independent manganese photooxidation sites in PSII. Initial estimates for V_{max} and K_m at each site were obtained, respectively, from the *x*-intercepts and −1/slope for each line. Final estimates were determined as described under Materials and Methods and are given in the text.

mined from the titration of DCIP photoreduction rates by the addition of either $MnCl_2$ or DPC, separately. Rates of DCIP photoreduction were measured as described under Materials and Methods. Figure 6A shows the rate of DCIP photoreduction as a function of added DPC. Kinetic parameters for DPC photooxidation were obtained by using an Eadie−Hofstee plot, as shown in Figure 6B. The plot indicates two distinct linear regions, suggesting two independent sites for DPC photooxidation in PSII (Segel, 1993), as described previously (Blubaugh & Cheniae, 1990). Initial estimates of K_m and V_{max} values at the two sites were obtained, respectively, from the inverse of the slopes and the *x*-intercepts of the two straight lines drawn through the data points in the Eadie−Hofstee plots. These estimates were used in an iterative process (Spears et al., 1971) to calculate actual kinetic parameters for DPC photooxidation at two sites in PSII (Blubaugh & Cheniae, 1990; Ghirardi & Seibert, 1992). The final estimates are $V_{max} = 22.5$ μmol of DCIP·(mg of Chl)$^{-1}$·h^{-1} and $K_m = 40$ μM for the high-affinity site, and $V_{max} = 85$ μmol of DCIP·(mg of Chl)$^{-1}$·h^{-1} and $K_m = 1200$ μM for the low-affinity site. The estimated K_ms agree very well with those reported by Blubaugh and Cheniae (1990). The accuracy of the estimated K_ms and V_{max}s was checked by fitting the experimental data to the two-enzyme Michaelis−Menten equation (eq 4). The lines through the data points in Figure 6A show the calculated fit.

A similar procedure was used to determine kinetic parameters for Mn^{2+} photooxidation by PSII. Figure 7A shows the rate of DCIP reduction as a function of added $MnCl_2$. Initial estimates of K_m and V_{max} for Mn^{2+} were obtained from the Eadie−Hofstee plot shown in Figure 7B. These estimates were used as described above to calculate the actual values of K_m and V_{max} associated with Mn^{2+} photooxidation at two sites in PSII. These values are $V_{max} = 3.8$ μmol of DCIP·(mg of Chl)$^{-1}$·h^{-1} and $K_m = 1.5$ μM for the high-affinity site, and $V_{max} = 37$ μmol of DCIP·(mg of Chl)$^{-1}$·h^{-1} and $K_m = 225$ μM for the low-affinity site. Figure 7A also shows the fit of the experimental data to the estimated kinetic parameters for Mn^{2+}.

These estimated parameters were used to generate the curves shown in Figure 5, according to the models described in the text.

REFERENCES

Ananyev, G. M., Shafiyev, M. A., Isayenko, R. V., & Klimov, V. V. (1988) *Biophysics 33*, 285−289.

Arnon, D. I. (1949) *Plant Physiol. 24*, 1−5.

Babcock, G. T., & Sauer, K. (1975) *Biochim. Biophys. Acta 396*, 48−62.

Barry, B. (1993) *Photochem. Photobiol. 57*, 179−188.

Blubaugh, D. J., & Cheniae, G. M. (1990) *Biochemistry 29*, 5109−5118.

Blubaugh, D. J., & Cheniae, G. M. (1992) in *Research in Photosynthesis* (Murata, N., Ed.) Vol. 2, pp 361−364, Kluwer Academic Publishers, Dordrecht, The Netherlands.

Blubaugh, D. J., Atamian, M., Babcock, G. T., Golbeck, J. H., & Cheniae, G. M. (1991) *Biochemistry 30*, 7586−7597.

Boerner, R. J., Nguyen, A. P., Barry, B. A., & Debus, R. J. (1992) *Biochemistry 31*, 6660−6672.

Buser, C. A., Thompson, L. K., Diner, B. A., & Brudvig, G. W. (1990) *Biochemistry 29*, 8977−8985.

Cheniae, G. M. (1980) *Methods Enzymol. 69*, 349−363.

Cheniae, G. M., & Martin, I. F. (1970) *Biochim. Biophys. Acta 197*, 219−239.

Cheniae, G. M., & Martin, I. F. (1971) *Plant Physiol. 47*, 568−575.

Chu, H.-A., Nguyen, A. P., & Debus, R. J. (1994a) *Biochemistry 33*, 6137−6149.

Chu, H.-A., Nguyen, A. P., & Debus, R. J. (1994b) *Biochemistry 33*, 6150−6157.

Chu, H.-A., Nguyen, A. P., & Debus, R. J. (1995) *Biochemistry 34*, 5859−5882.

Coleman, W. J., & Govindjee (1987) *Photosynth. Res. 13*, 199−223.

Debus, R. J. (1992) *Biochim. Biophys. Acta 1102*, 269−352.

Debus, R. J., Barry, B. A., Sithole, I., Babcock, G. T., & McIntosh, L. (1988) *Biochemistry 27*, 9071−9074.

Dekker, J. P., Van Gorkom, H. J., Wensink, J., & Ouwehand, L. (1984) *Biochim. Biophys. Acta 767*, 1−9.

Diner, B. A., & Nixon, P. J. (1992) *Biochim. Biophys. Acta 1101*, 134−138.

Dismukes, G. C. (1986) *Photochem. Photobiol. 43*, 99−115.

Dismukes, G. C. (1988) *Chem. Scr. 28A*, 99−104.

Ghirardi, M. L., & Seibert, M. (1992) in *Research in Photosynthesis* (Murata, N., Ed.) Vol. 2, pp 357−360, Kluwer Academic Publishers, Dordrecht, The Netherlands.

Ghirardi, M. L., Lutton, T. W., & Seibert, M. (1995) in *Proceedings of the Xth International Photosynthesis Congress* (in press).

Hoganson, C. W., Ghanotakis, D. F., Babcock, G. T., & Yocum, C. F. (1989) *Photosynth. Res. 22*, 285−293.

Hoganson, C. W., Casey, P. A., & Hansson, O. (1991) *Biochim. Biophys. Acta 1057*, 399−406.

Joliot, P., & Joliot, A. (1984) *Biochim. Biophys. Acta 765*, 210−218.

Klimov, V. V., Allakhverdiev, S. I., Shuvalov, V. A., & Krasnovsky, A. A. (1982) *FEBS Lett. 148*, 307−312.

Kramer, D. M., & Crofts, A. R. (1990) *Photosynth. Res. 23*, 231−240.

Kuwabara, T., & Murata, N. (1983) *Plant Cell Physiol. 24*, 741−747.

Leatherbarrow, R. J. (1992) *GraFit Version 3.0*, Erithacus Software Ltd., Staines, U.K.

Metz, J. G., Pakrasi, H. B., Seibert, M., & Arntzen, C. J. (1986) *FEBS Lett. 205*, 269−274.
Metz, J. G., Nixon, R. J., Rögner, M., Brudvig, G. W., & Diner, B. A. (1989) *Biochemistry 28*, 6960−6969.
Miller, M., & Cox, R. P. (1983) *FEBS Lett. 155*, 331−333.
Miller, M., & Brudvig, G. W. (1990) *Biochemistry 29*, 1385−1392.
Mohanty, N., Vass, I., & Demeter, S. (1989) *Physiol. Plant. 76*, 386−390.
Nixon, P. J., & Diner, B. A. (1992) *Biochemistry 31*, 942−948.
Nixon, P. J., Trost, J. T., & Diner, B. A. (1992) *Biochemistry 31*, 10859−10871.
Ono, T., & Inoue, T. (1983) *FEBS Lett. 164*, 255−260.
Packham, N. K., & Barber, J. (1984) *Biochim. Biophys. Acta 764*, 17−23.
Preston, C., & Seibert, M. (1989) *Photosynth. Res. 22*, 101−113.
Preston, C., & Seibert, M. (1990) in *Current Research in Photosynthesis* (Baltscheffsky, M., Ed.) Vol. I, pp 925−928, Kluwer Academic Publishers, Dordrecht, The Netherlands.
Preston, C., & Seibert, M. (1991a) *Biochemistry 30*, 9615−9624.
Preston, C., & Seibert, M. (1991b) *Biochemistry 30*, 9625−9633.
Rashid, A., Bernier, M., Pazdernick, L., & Carpentier, R. (1991) *Photosynth. Res. 30*, 123−130.
Segel, I. W. (1993) in *Enzyme kinetics—Behavior and analysis of rapid equilibrium and steady-state enzyme systems*, John Wiley & Sons, New York.
Seibert, M. (1993) in *The Photosynthetic Reaction Center* (Deisenhofer, J., & Norris, J. R., Eds.) Vol. I, pp 319−356, Academic Press, New York.
Seibert, M., Tamura, N., & Inoue, Y. (1989) *Biochim. Biophys. Acta 974*, 185−191.
Spears, G., Sneyd, J. G. T., & Loten, E. G. (1971) *Biochem. J. 125*, 1149−1151.
Styring, S., & Rutherford, A. W. (1987) *Biochemistry 26*, 2401−2405.
Tamura, N., & Cheniae, G. (1987) *Biochim. Biophys. Acta 890*, 179−194.
Tamura, N., Ikeuchi, M., & Inoue, Y. (1989) *Biochim. Biophys. Acta 973*, 281−289.
Thompson, L. K., & Brudvig, G. W. (1988) *Biochemistry 27*, 6653−6658.
Tripathy, B. C., Bhatia, B., & Mohanty, P. (1983) *Biochim. Biophys. Acta 722*, 89−93.
Vermaas, W. F. J., Ikeuchi, M., & Inoue, Y. (1988) *Photosynth. Res. 17*, 97−113.
Whitelegge, J. P., Koo, D., Diner, B. A., Domian, I., & Erickson, J. M. (1995) *J. Biol. Chem. 270*, 225−235.
Yamashita, T., & Butler, W. L. (1968) *Plant Physiol. 43*, 1978−1986.

BI951657D